

Manganese Stabilizing Protein of Photosystem II Is a Thermostable, Natively Unfolded Polypeptide[†]

Nikos Lydakis-Simantiris,[‡] Ronald S. Hutchison,[§] Scott D. Betts,^{‡,||} Bridgette A. Barry,[§] and Charles F. Yocum^{*,‡,⊥}

Department of Biology and Department of Chemistry, The University of Michigan, Ann Arbor, Michigan 48109-1048, and
Department of Biochemistry, Molecular Biology and Biophysics, University of Minnesota, St. Paul, Minnesota 55108

Received July 31, 1998; Revised Manuscript Received October 19, 1998

ABSTRACT: The thermostability of manganese stabilizing protein of photosystem II was examined by biochemical and spectroscopic techniques. Samples of both native and recombinant spinach manganese stabilizing protein incubated at 90 °C and then cooled to 25 °C were capable of rebinding to, and of reactivating, the O₂-evolution activity of photosystem II membranes from which the native protein had been removed. Far-UV circular dichroism and FT-IR spectroscopies were used to analyze the structural consequences of heating manganese stabilizing protein. The data obtained from these techniques show that heating causes a complete loss of the protein's secondary structure, and that this is a reversible, noncooperative phenomenon. Upon cooling, the secondary structures of the heat-treated proteins return to a state similar to, but not identical with, that of the native, unheated controls. Restoration of a near-native tertiary structure is confirmed both by size-exclusion chromatography and by near-UV circular dichroism. The functional and structural thermostability of manganese stabilizing protein reported here, in conjunction with additional known properties of this protein (acidic pI, high random coil and turn content, anomalous hydrodynamic behavior), identifies manganese stabilizing protein as a natively unfolded protein [Weinreb et al. (1996) *Biochemistry* 35, 13709–13715]. Although these proteins lack amino acid sequence identity, their functional solution conformations under physiological conditions are said to be "natively unfolded". We suggest that, as with other members of this family of proteins, the natively unfolded structure of manganese stabilizing protein facilitates the highly effective protein–protein interactions that are necessary for its assembly into photosystem II.

Oxidation of water and release of O₂ as a byproduct during the photosynthetic conversion of light to chemical energy take place in the O₂-evolving complex (OEC)¹ of PSII of higher plants, algae, and cyanobacteria (for reviews, see 1–3). This process occurs via five distinct redox states, known as S_n states (*n* = 0–4) (4). Photosystem II consists of several intrinsic proteins that have been shown to ligate the antenna and reaction center chlorophylls as well as other redox active cofactors that participate in primary and secondary electron-transfer reactions (2, 5). These species

include the core, Chl *a*-binding antenna proteins called CP47 and CP43, the α and β subunits of cytochrome *b*₅₅₉, and the reaction center polypeptides known as D1 and D2. Three water-soluble proteins with apparent molecular masses of 17, 23, and 33 kDa are also necessary for efficient O₂ evolution by PSII in eukaryotic organisms (for reviews, see 2, 6, 7). The polypeptides of PSII provide the ligation environment for a cluster of four manganese atoms which serves as a substrate–H₂O binding site and as the accumulator of the 4 oxidizing equiv which are needed for the oxidation of two H₂O molecules to O₂ (8). In addition to Mn, one atom each of Ca²⁺ and Cl[–] is necessary for the redox cycling that oxidizes H₂O (1, 9–12).

In the intact enzyme system, PSII extrinsic proteins regulate the integrity of the OEC (6). The 23 and 17 kDa proteins facilitate retention of Ca²⁺ and Cl[–] at the sites from which they regulate Mn redox activity, and the 33 kDa protein, also called MSP (manganese stabilizing protein), is responsible for maintaining the stability and efficient turnover of the tetranuclear manganese cluster (6, 7). In the absence of MSP, two of the four manganese atoms of the OEC are released into solution as Mn²⁺ (13). This phenomenon is not observed if MSP-depleted PSII is exposed to high (≥ 100 mM) Cl[–] concentrations (13). However, removal of MSP also lowers the O₂-evolution activity of PSII by approximately 60% (14). Thermoluminescence and O₂-evolution studies on MSP-depleted preparations have shown that

[†] This research was supported by grants from the National Science Foundation Molecular Biochemistry Program to C.F.Y. (MCB 97-27777) and the National Science Foundation Molecular Biophysics Program to B.A.B. (MCB 98-08934).

*Corresponding author: Department of Biology, University of Michigan, Ann Arbor, MI 48109-1048. Telephone: (734)-647-0887. FAX: (734)-647-0884. E-mail: cyocum@umich.edu.

[‡] Department of Biology, The University of Michigan.

[§] Department of Biochemistry, Molecular Biology and Biophysics, University of Minnesota.

^{||} Present address: Department of Biology, Massachusetts Institute of Technology, Cambridge, MA 02139.

[⊥] Department of Chemistry, The University of Michigan.

¹ Abbreviations: Bis-Tris, bis(2-hydroxyethyl)iminotris(hydroxymethyl)methane; CD, circular dichroism; Chl, chlorophyll; CP43, CP47, chlorophyll *a*-binding antenna proteins with molecular masses of 43 and 47 kDa, respectively; FT-IR, Fourier transform infrared spectroscopy; MES, 2-(*N*-morpholino)ethanesulfonic acid; MSP, manganese stabilizing protein; OEC, oxygen-evolving complex; PS, photosystem; SDS–PAGE, sodium dodecyl sulfate–polyacrylamide gel electrophoresis; Tris, tris(hydroxymethyl)aminomethane; UV, ultraviolet.

the S-state cycle is modified; S_2 and S_3 exhibit increased stability, and the $S_3 \rightarrow S_4 \rightarrow S_0$ transition becomes slower by a factor of 3–5, depending on the preparation under investigation (15–17).

Biochemical analyses have revealed that there are two copies of MSP per PSII reaction center (18–20, but see 21), although the binding sites for both copies have not been completely characterized. Cross-linking studies (22, 23) demonstrate binding of MSP to the E loop of the core antenna protein CP47, and limited proteolysis (24) and biotinylation (25) studies are in agreement with this conclusion. Site-directed mutagenesis also showed that the E loop of CP47 participates in MSP binding to PSII (26, 27). Based on experiments using limited proteolysis with trypsin, Enami and co-workers (28) have recently suggested that additional binding sites for MSP may reside on CP43 and on cytochrome b_{559} polypeptides.

Several proposals have been made concerning the function of MSP. The observation that exposure of PSII to high concentrations of Tris buffer caused simultaneous dissociation of MSP and the tetranuclear Mn cluster from PSII led to the proposal that MSP might provide Mn ligands (29), but later work showed that Cl^- (100 mM) will maintain the integrity of the Mn cluster in the absence of MSP (13). Participation of MSP in oxidation of Mn^{2+} during photoactivation has been suggested as well (30). Based on some of the similarities between the effects of MSP depletion and of Cl^- depletion on PSII, Bricker and Frankel (7) have proposed that the main function of MSP is to regulate the Cl^- –Mn interaction by maintaining Cl^- at an adequate concentration in the vicinity of OEC. Betts et al. (20) used the competition between mutant MSP (V235A) and the native spinach or *Arabidopsis* proteins to show that optimal restoration of function and stability to the OEC required more than one copy of bound MSP per PSII reaction center. Taking into account the proposed pseudo C_2 symmetry of the PSII reaction center, they suggested that one copy of MSP regulates O_2 evolution activity whereas the other copy provides structural support that stabilizes the Mn cluster.

Studies of the secondary structure of spinach MSP in solution using CD spectroscopy have shown that it is predicted to contain a relatively small amount of α -helix (<10%) and a larger amount of β -sheet (>35%); turns and random coil conformations comprise the remainder (~50%) of the predicted secondary structure (31, 32). Characterization of MSP from the thermophilic cyanobacterium *Synechococcus elongatus* produced data that were used to predict a higher percentage of α -helix (33) than has been predicted for mesophilic MSP. Differences in the proposed secondary structure content of the two proteins may be related to their relatively limited amino acid sequence identity (34). When the heat labilities of the secondary structures of MSP from spinach and *Synechococcus* were compared, *Synechococcus* MSP, as expected, retained its secondary structural components at much higher temperatures than did the spinach protein. However, no information about the functional thermostability of spinach MSP was reported in this study (34).

We have used FT-IR spectroscopy to show that the secondary structure of MSP in solution can vary over a wide range of values, rather than being fixed (35). However, the β -sheet component of MSP seems to increase at the expense

of unordered conformations upon functional rebinding of the protein to PSII (35). Here we present data showing that recombinant and native spinach MSP are thermostable proteins which are capable of recovering a substantial fraction (>80%) of their native, functional state after prolonged treatment at high temperatures. Far-UV CD and FT-IR spectroscopies yield data showing that spinach MSP incubated at high temperature recovers a substantial portion of its secondary structure when cooled to room temperature. Near-UV CD and size-exclusion chromatography data show that the tertiary structure of the protein is also recovered. These results, taken together with the high percentage of turns and random coil predicted from several studies, including our own, indicate that MSP is a member of a family of “natively unfolded” proteins (36).

MATERIALS AND METHODS

Preparation of PSII Membranes, Extraction of Native MSP, and Assay of O_2 Evolution Activity. PSII membranes were isolated from fresh market spinach according to the method described in (37) with modifications described in (38). For extraction of the 17 and 23 kDa extrinsic polypeptides, PSII membranes were incubated in the dark with 2 M NaCl for 0.5–1 h on ice as described in (39). MSP was extracted from NaCl-washed PSII membranes by incubation in the dark in 50 mM MES (pH 6.0), 2.6 M urea, 200 mM NaCl for 0.5–1 h on ice (39). The sample was then centrifuged (40000g, 30 min); the pellet was resuspended in 50 mM MES (pH 6.0), 200 mM NaCl, and then washed once in the same buffer. The supernatant contained almost pure MSP, and was subjected to further purification (see below). The O_2 -evolution activities of PSII samples were assayed with a Clark-type oxygen electrode; 15 μ g of Chl was added to a medium containing 0.4 M sucrose, 60 mM $(CH_3)_4NCl$, 20 mM $CaCl_2$, and 50 mM MES (pH 6.0); 600 μ M 2,6-dichloro-*p*-benzoquinone was used as the electron acceptor. Typical sample activities were the following: intact PSII, 500–600 μ mol of O_2 (mg of Chl) $^{-1}$ h $^{-1}$; NaCl-washed PSII, 420–500 μ mol of O_2 (mg of Chl) $^{-1}$ h $^{-1}$; urea–NaCl-washed PSII, ~200 μ mol of O_2 (mg of Chl) $^{-1}$ h $^{-1}$.

Preparation and Purification of Native and Recombinant MSP. The supernatant containing native MSP extracted from PSII was recentrifuged (40000g, 30 min), and then two sequential 5 h dialysis steps were carried out, the first against 100 mM Tris (pH 8.0), 10 mM NaCl and the second against 50 mM MES (pH 6.0), 10 mM NaCl. The dialyzed protein was diluted with an equal volume of 50 mM MES (pH 6.0), 10 mM NaCl, 5% betaine (buffer MES-A). After centrifugation (40000g, 20 min), the dialysate was loaded on a Resource-Q column (Pharmacia Biotech) equilibrated with the dilution buffer. A step gradient (30 mM, 150 mM, and 500 mM NaCl) was then applied. Concentrated, purified native MSP was eluted at 150 mM NaCl. For FT-IR experiments, native MSP was purified by an adaptation of the method of Kuwabara et al. (40). Extracted MSP was dialyzed against 20 mM sodium phosphate, pH 6.6, loaded onto a DEAE-Sepharose column, and eluted with 60 mM NaCl in dialysis buffer. For recombinant wild-type MSP, *E. coli* transformation and gene expression were done as described in (41). Cells were sonicated, and the MSP inclusion bodies containing processed, mature MSP were isolated, washed, and then solubilized with 3 M urea.

Insoluble material was removed by centrifugation, and the resulting MSP was purified from the supernatant fraction by two chromatographic steps. First, a linear gradient (10–250 mM NaCl) was applied to a Resource-Q column equilibrated with 20 mM Bis-Tris (pH 6.4), 3 M urea, 10 mM NaCl (41). Partially purified MSP eluted at about 120 mM NaCl. This eluate was then loaded onto a Mono-Q column (Pharmacia, HR 5/5), equilibrated with MES-A buffer, and a step gradient (30 mM, 100 mM, and 500 mM NaCl) was applied. Purified MSP eluted at 100 mM NaCl. Samples of MSP purified by all methods used here appeared as single bands on SDS–polyacrylamide gels (not shown). The integrity of the *N*-terminus of native and recombinant samples was examined by Edman degradation; in both cases, the expected sequence (EGGKR) was found (42).

Structural and Functional Analyses of MSP. Changes in the secondary structure of MSP as a function of temperature were examined by far-UV CD and FT-IR spectroscopies. All MSP samples tested by CD spectroscopy were transferred first to 10 mM KH₂PO₄ (pH 6.0) by extensive dialysis. Protein concentration was determined using an extinction coefficient of 16 mM⁻¹·cm⁻¹ (18). An AVIV 62DS spectrometer controlled by a 486 microcomputer was used, and the measurements were done essentially as described in (43). Before initiation of data acquisition, the instrument was calibrated with (+)-10-camphorsulfonic acid (1 mg/mL in H₂O) as described in (44). The temperature at the cuvette chamber was controlled within 0.1 °C accuracy, and samples were thermally equilibrated before data acquisition. Instrumental conditions are given in the figure legends. Circular dichroism spectra were simulated with various programs [SELCON, VARSLC, CONTIN (45)] kindly provided by Dr. Norma Greenfield (Neuroscience and Cell Biology Department, Robert Wood Medical School, Piscataway, NJ). Results of the simulations were used to extract predictions of the content of α -helix, β -sheet, turns, and random coil structures in soluble MSP. Near-UV CD spectroscopy utilized MSP samples in 10 mM KH₂PO₄ (pH 6.0); these were transferred to a 1 cm cuvette, and spectra from 250 to 330 nm were recorded. Other experimental conditions are described in the figure legend.

For FT-IR spectroscopy, MSP was transferred to a D₂O buffer, containing 5 mM MES–NaOD, pD 6.0. The pD is reported as the uncorrected meter reading (46). FT-IR spectra were obtained as previously described (35). Temperature changes were achieved through the use of a Harrick variable-temperature cell and a recirculating water bath, as previously described (47). The temperature was controlled to ± 1.0 °C. Spectral conditions were as follows: resolution, 2 cm⁻¹; apodization function, Happ–Genzel; interferograms, double-sided; zero-filling, one level; mirror velocity, 2.5 cm/s; mirror scans, 2000. Protein concentrations were in the range from 90 to 580 μ M. The sample (6 μ L) was placed between two CaF₂ windows using a 6 μ m spacer. A buffer spectrum was recorded, and this spectrum was subtracted from protein spectra recorded on the same day. Band narrowing analysis, through Fourier deconvolution and second-derivative analysis, was performed using Omnic (Nicolet Instruments, Madison, WI) and Grams (Galactic Industries Co., Salem, NH) software. The deconvolution parameters were the following: *K*, 2; line width, 40 cm⁻¹; apodization function, modified Happ–Genzel. Second-derivative analysis was

performed with a Savitsky–Golay procedure, and regression analysis was performed with Gaussian spectral components.

Changes in the tertiary structure of MSP were determined using size-exclusion chromatography and near-UV CD spectroscopy. A Superose-12 column (Pharmacia, HR 10/30) equilibrated with 50 mM Bis-Tris (pH 6.4), 100 mM NaCl was connected to a Pharmacia FPLC system. Blue dextran (MW $\geq 2 \times 10^6$) was used to determine the void volume of the column, and aprotinin (6.5 kDa), cytochrome *c* (12.4 kDa), carbonic anhydrase (29 kDa), and bovine serum albumin (66 kDa) were used to calibrate the column and for construction of a linear standard curve that plots the log of the molecular masses of standard proteins as a function of their elution volumes. The apparent molecular masses of MSP samples were determined from the calibration curve.

Urea/200 mM NaCl washed PSII membranes were reconstituted with either native or recombinant wild-type samples of MSP that had been previously incubated either at room temperature or at 90 °C for various times; reconstitution mixtures containing 0.5–5 mol of MSP per mole of PSII were incubated at room temperature for 1 h as described in (39). Estimations of PSII and MSP concentrations were based on the assumption of 250 Chl per reaction center in PSII membranes (37) and an extinction coefficient of 16 mM⁻¹ cm⁻¹ (18), respectively. The O₂ evolution activity of reconstituted PSII samples was measured at 25 °C by a Clark-type electrode. Assay conditions were the same as described in the sample preparation section. The rate of oxygen evolution was measured under saturating light conditions, whereas the total production of O₂ in 4 min was measured under 80% light saturation. In combination, these assays monitor the rate of enzyme turnover and the extent to which rebinding of MSP restores the long-term stability of the reconstituted system.

The amount of rebinding of MSP to PSII was determined by SDS–polyacrylamide gel electrophoresis (10% acrylamide, 4.7 M urea) using the Neville buffer system (48). For details about electrophoresis conditions, see (39). The relative amount of MSP bound to PSII was estimated by integration of the Coomassie-stained MSP bands by using Sigmagel software (Jandel Scientific). NaCl-washed PSII was present on the gel as a control (100% MSP bound). For consistency, MSP band integrals were normalized to the integral of the Coomassie-stained 47 kDa band. For data analysis, Origin v4.1 (Microcal Software, Inc.) was used.

RESULTS

MSP Reactivates O₂ Evolution after Exposure to High Temperature. As a result of characterizations of truncation mutations at the C-terminus of recombinant spinach MSP, we discovered that the wild-type and mutant proteins yielded anomalously high molecular masses upon elution from a gel filtration column (49). One explanation for this result might be that MSP is a natively unfolded protein (36). Such proteins resemble MSP in that they often have acidic pI's, have anomalous hydrodynamic properties, and exhibit a resistance to irreversible denaturation by heat, even though they are, like spinach MSP, derived from mesophilic organisms (36). Unlike proteins isolated from thermophiles, whose secondary structures are resistant to disruption by heating to high temperatures (≥ 80 –90 °C), natively unfolded proteins lose

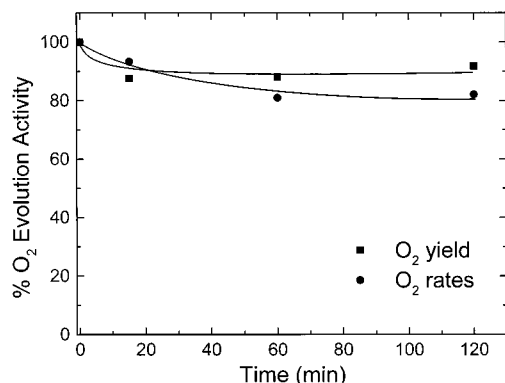


FIGURE 1: Recovery of O₂-evolution activity of PSII membranes reconstituted with recombinant, wild-type MSP incubated at 90 °C for 0, 15, 60, and 120 min. For rebinding to PSII, a stoichiometry of 3 mol of MSP/mol of PSII was used. The points shown represent the average of activities obtained from three separate experiments; the error in the measurements was $\pm 5\%$. The control (0 min) sample corresponds to recombinant MSP incubated at room temperature for 15 min before mixing with urea, salt-washed PSII membranes, and it was used as control [100% O₂ evolution was $420\text{--}500 \mu\text{mol}$ of O₂ (mg of Chl)⁻¹ h⁻¹; 100% O₂ yield was $16 \mu\text{mol}$ of O₂ (mg of Chl)⁻¹ (4 min)⁻¹].

secondary structure upon heating to lower temperatures [for example, see (50)]. Figure 1 shows the effect on O₂ evolution activity of heating recombinant wild-type spinach MSP at 90 °C for periods of time up to 2 h. Results for activity

restored by reconstitution of PSII with 3 mol of heated, recombinant wild-type MSP per mole of PSII are presented. Loss of about 10–20% of MSP activity occurred very rapidly (in less than 15 min of incubation), but the substantial (ca. 80%) amount of remaining activity was stable for up to 2 h at 90 °C. From these data it is apparent that restoration of PSII activity by rebinding of MSP is nearly independent of the time of incubation at high temperature, up to 2 h. Results similar to those shown in Figure 1 were obtained with native MSP (data not shown).

To characterize the effect of heat treatment on MSP in greater detail, we examined the ability of heated proteins to rebind to urea, salt-washed PSII membranes at several MSP/PSII ratios, and assayed restoration of function in the reconstituted system. Because Figure 1 shows that any deleterious effects of high-temperature incubation occur in less than 15 min, this incubation time was employed for all subsequent experiments. Figures 2 and 3 show the rebinding and reactivating capacity of both native and recombinant MSP incubated for 15 min either at room temperature (panels A) or at 90 °C (panels B). Stoichiometric rebinding of MSP to urea, salt-washed PSII membranes was achieved after mixing 2 mol of unheated native MSP with 1 mol of PSII as described under Materials and Methods (Figure 2A, diamonds). In the case of recombinant MSP incubated at room temperature (Figure 3A), a slight excess of MSP

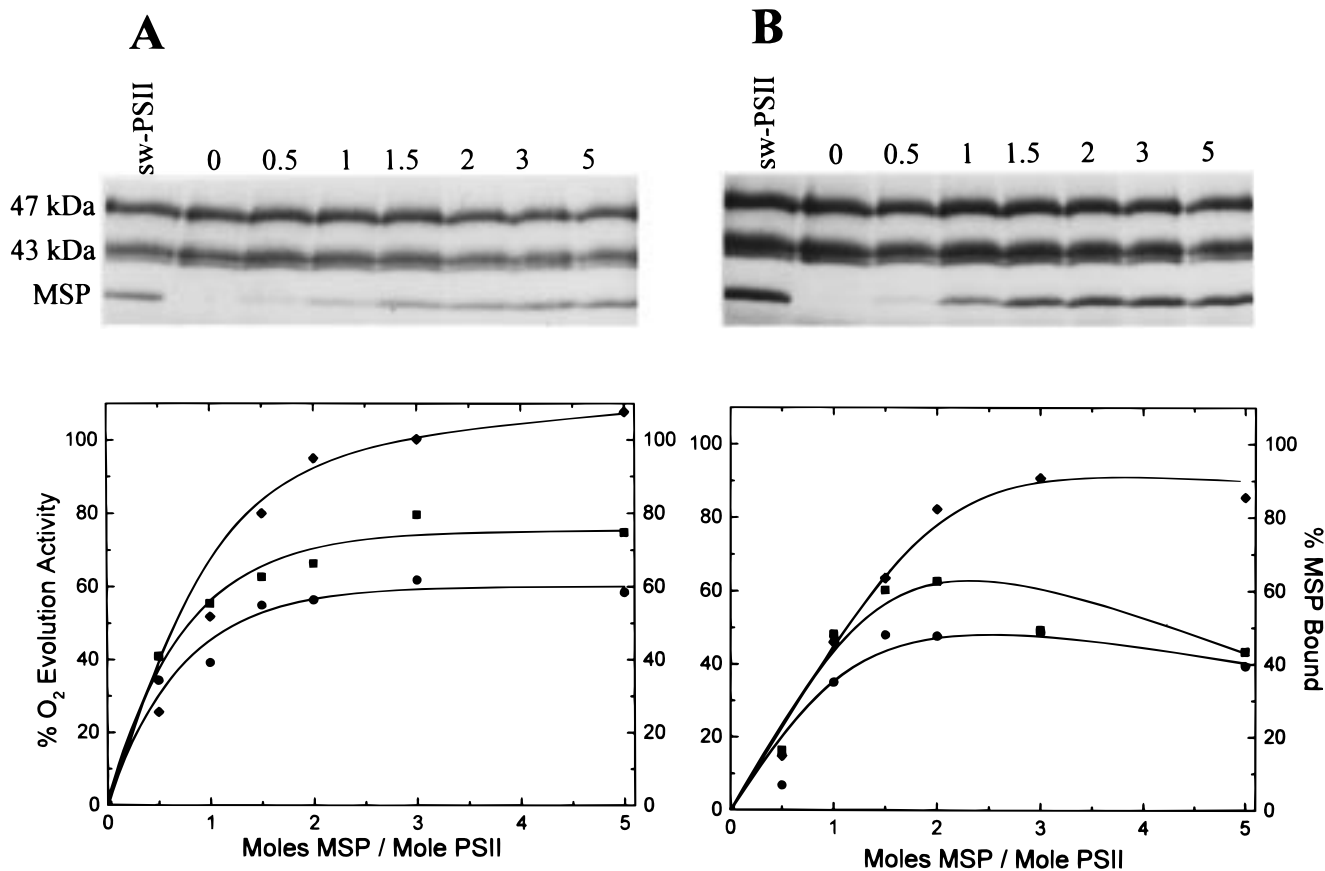


FIGURE 2: Reconstitution of PSII with native MSP, incubated for 15 min at room temperature (panel A) or at 90 °C (panel B). Rebinding curves (diamonds) were plotted with data from densitometric analysis of the gels shown. Differences in band intensities reflect differences in staining in different electrophoresis experiments. The integrated intensity of the CP47 band was used to normalize MSP concentrations in individual samples. Numbers indicate moles of MSP per mole of PSII in the reconstitution mixture. Oxygen evolution activity rates (circles) and total oxygen yield in 4 min under nonsaturating illumination (squares) were obtained from unwashed, reconstituted samples as described under Materials and Methods. The 100% activities and other conditions were as given in the legend to Figure 1. The 100% bound MSP corresponds to the amount of MSP bound to a salt-washed PSII membrane preparation (2 mol MSP/mol of PSII).

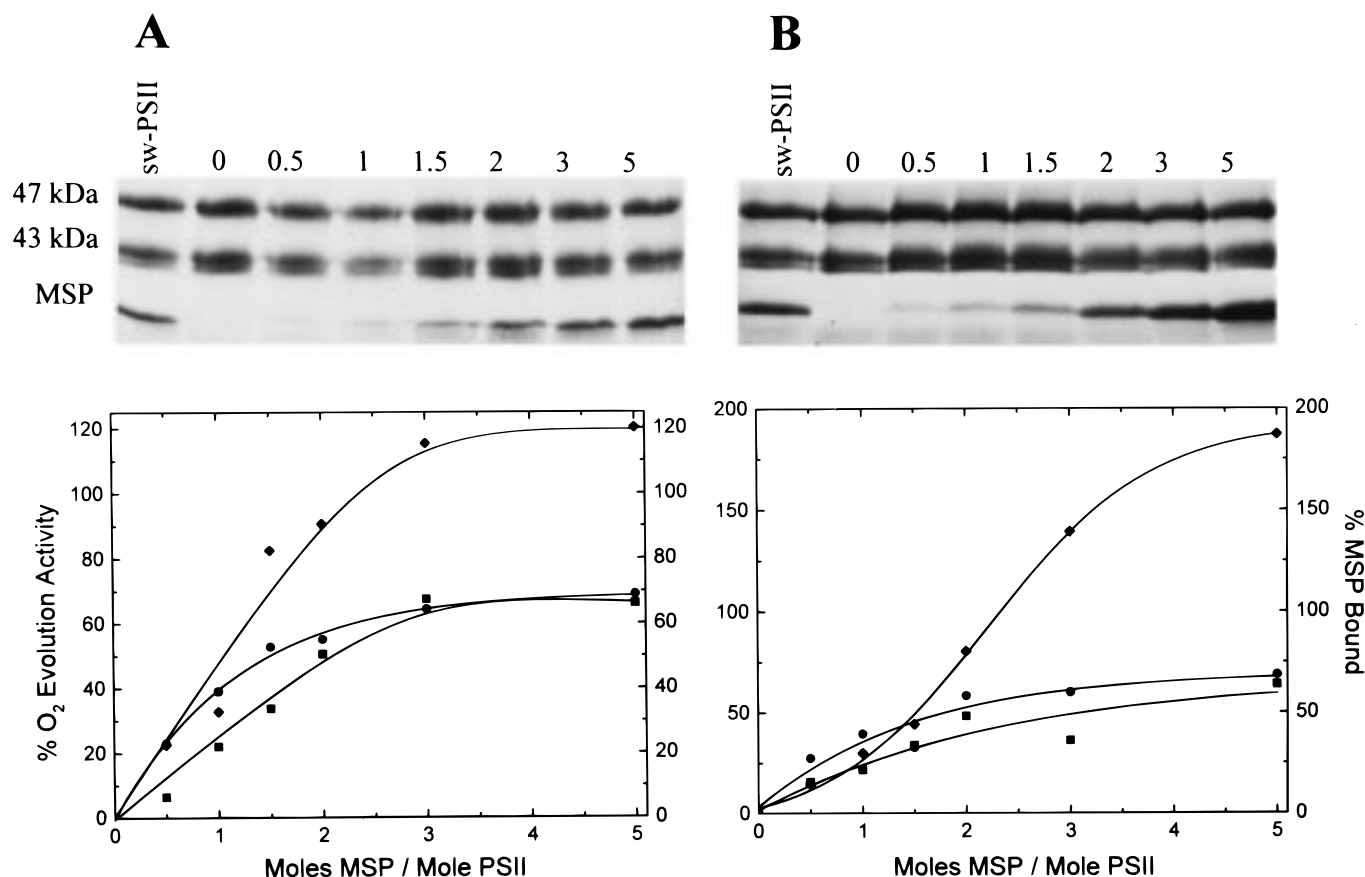


FIGURE 3: Reconstitution of PSII with recombinant, wild-type MSP, incubated for 15 min at room temperature (panel A) or at 90 °C (panel B). Data analyses, experimental procedures, and 100% control activities are given in the legend to Figure 2 and under Materials and Methods.

binding to PSII (about 20% higher than salt-washed PSII membranes) was revealed by densitometric analysis of Coomassie-stained SDS-PAGE gels. This binding anomaly has been observed in previous studies (43). On the other hand, binding of recombinant MSP that had been incubated at 90 °C (Figure 3B) approached 200% of control levels. We attribute this behavior to adventitious MSP binding that may be due to partial changes in secondary and/or tertiary structure. In addition, the binding curve for heated, recombinant MSP is sigmoidal whereas the binding data in all other reconstitution experiments can be fitted by hyperbolas. The apparent lack of sigmoidicity in binding curves presented in previous studies has been attributed to the very high affinity of MSP for both of its binding sites (19). Figure 3 shows that binding of heated recombinant MSP to PSII, although sigmoidal in nature, restores O₂ evolution activity to high levels in samples reconstituted with 2 mol of MSP/mol of PSII, suggesting that any alteration in binding affinity by heating is insufficient to interfere with reconstitution of the OEC. Reconstitution of PSII with heated MSP, native or recombinant, resulted in slightly lower activity as compared to MSP incubated at room temperature, in agreement with the results in Figure 1. The presence of high concentrations (>3 mol of MSP/mol of PSII) of heated, native MSP during activity assays can cause modest inhibitory effects on PSII turnover (Figure 3B). In all reconstitution experiments, however, saturation of O₂ evolution activity occurred at about 2 mol of MSP/mol of PSII, a stoichiometry that agrees with previous results (18, 20, 39). The ability of normal stoichi-

ometries of both native and recombinant heated MSP species to restore high levels of O₂ evolution activity after rebinding to PSII indicates that these proteins are resistant to irreversible denaturation, in terms both of rebinding to PSII and of ability to reactivate the OEC.

Spectroscopic Characterization of Effects of Temperature on MSP Secondary Structure. The effects of heating on MSP secondary structure were examined by far-UV CD and by FT-IR spectroscopy. Figures 4 and 5 present CD spectra of native and recombinant MSP samples, respectively, acquired at several temperatures. The CD spectra of both proteins are seen to undergo a temperature-dependent transition in which the features attributed to α -helix and β -sheet are replaced by a featureless trough, indicative of the presence of large amounts of disordered structure (44, 51). Both figures include the CD spectra of MSP recorded at 25 °C after 1 h of incubation either at room temperature or at 90 °C. Results obtained for both MSP preparations exhibited reversible behavior; that is, CD spectra obtained before and after heating were similar. Incubation of MSP at 65 °C, instead of 90 °C, and cooling to 25 °C resulted in CD spectra indistinguishable from those obtained after incubation at 90 °C (data not shown), and incubation of heated MSP at 25 °C for an additional hour resulted in no further changes in the 25 °C CD spectra shown in Figures 4 and 5 (not shown). At 25 °C both MSP species produced CD spectra characteristic of proteins containing a small percentage of α -helix along with higher contents of β -sheet and random coil components, consistent with other investigations (31, 32). An analysis of

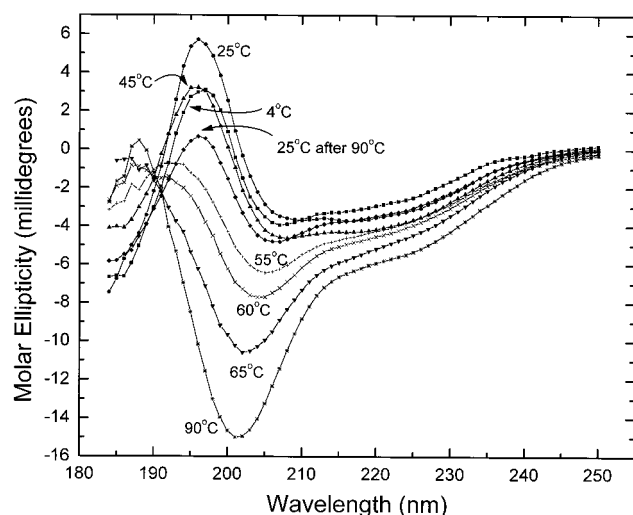


FIGURE 4: Far-UV CD spectra of native MSP in 10 mM KH_2PO_4 . MSP samples (11 μM) were thermally equilibrated at the indicated temperatures, and then 20 scans were averaged. Experimental conditions: time constant 1 s, bandwidth 1.5 nm, path length 0.1 cm, scan speed 30 nm/min. Secondary structure components predicted from analysis of these spectra are presented in Table 1.

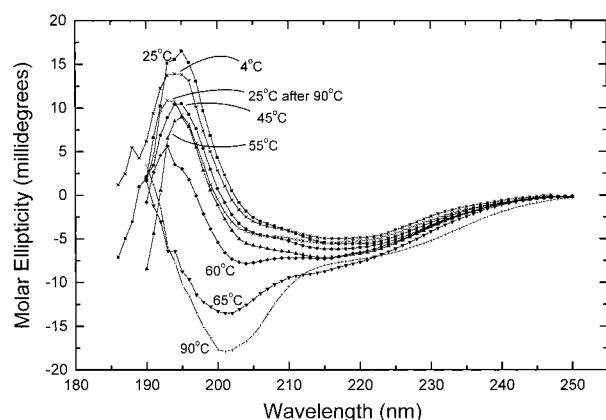


FIGURE 5: Far-UV CD spectra of recombinant, wild-type MSP in 10 mM KH_2PO_4 . MSP samples (11 μM) were thermally equilibrated at the indicated temperatures, and then 20 scans were averaged. Other experimental conditions are given in the legend to Figure 4.

Table 1: Predicted Secondary Structure Components of Native and Recombinant MSP Incubated at either 25 °C or 90 °C^a

MSP sample	% α -helix	% β -sheet	% turns, random coil	total
native, 25 °C	4	47	49	100
recombinant, 25 °C	7	44	45	96
native, 90 °C	8	30	55	93
recombinant, 90 °C	3	48	46	97

^a CD spectra were recorded at 25 °C before or after the heat treatment.

our CD data, as described under Materials and Methods, is shown in Table 1. These values are qualitatively similar to those reported by Xu et al. (31) and by Shutova et al. (32). However, two additional results are apparent from the data in this table. First, the predicted secondary structure contents of unheated native and recombinant MSP samples differ somewhat, and second, analyses of the CD spectra recorded at 25 °C after incubation for 1 h at 90 °C show that, relative to the unheated control proteins, the predicted contents of both α -helix and β -sheet were slightly altered (Table 1).

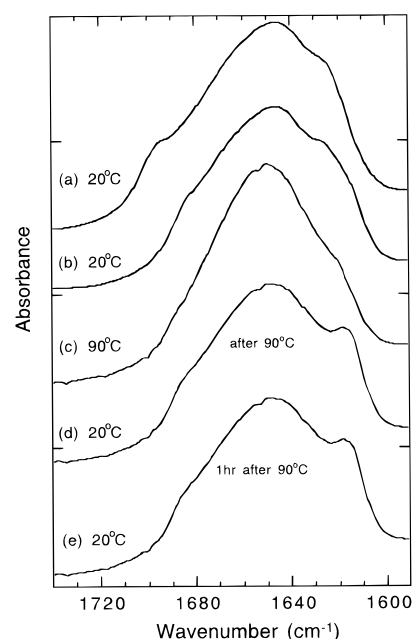


FIGURE 6: FT-IR spectrum, showing the amide I' band, obtained from native MSP samples at various temperatures. Spectra were obtained at 20 °C (a, b, d, and e) and at 90 °C (c). In (a) and (b), spectra were obtained from two different preparations of native MSP at 20 °C. In (b–e), spectra were obtained from one native MSP sample at 20 °C (b), after heating to 90 °C (c), immediately after cooling back to 20 °C (d), and after additional incubation of the heated sample for 1 h at 20 °C (e). The tick marks on the y axis represent 0.05 absorbance unit.

The extent of variability in MSP secondary structure, and structural consequences of heating were also examined by FT-IR spectroscopy. Variation in the secondary structure of native MSP was followed by analysis of the amide I', or C=O stretching, vibration of the peptide bond, which is sensitive to changes in hydrogen bonding and thus to alterations in secondary structure (52–55). This vibrational mode appears in the 1650 cm^{-1} region of the spectrum, but the exact frequency depends on the structure of the protein. Analyses of protein FT-IR spectra are often carried out in D_2O -containing buffers to eliminate a spectral contribution from water in the amide I' region. Correlations have been derived between the frequencies of spectral components in this region and known secondary structure motifs in proteins. Identification of amide I' spectral components is performed through band narrowing and regression analysis (52–54).

In Figure 6a,b, we present the amide I' line shape of native MSP samples; spectra were obtained at 20 °C. Differences are observed in the amide I' line shapes, when different preparations of MSP are compared (Figure 6a,b). This result is expected from our previous work, in which we showed that the solution structures of reconstitutively active MSP samples exhibited considerable variation (35). Upon heating to 90 °C, FT-IR spectra exhibit a significant narrowing of the amide I' band (Figure 6c). Cooling the sample results in the reversal of these thermally induced changes (Figure 6d). Further incubation at 20 °C does not significantly change the amide I' line shape (Figure 6e).

To quantitatively analyze these conformational changes, band narrowing analysis was performed (Figure 7A–C). Spectra were obtained on native MSP at 20 °C (Figure 7A), after heating that same sample to 90 °C (Figure 7B), and

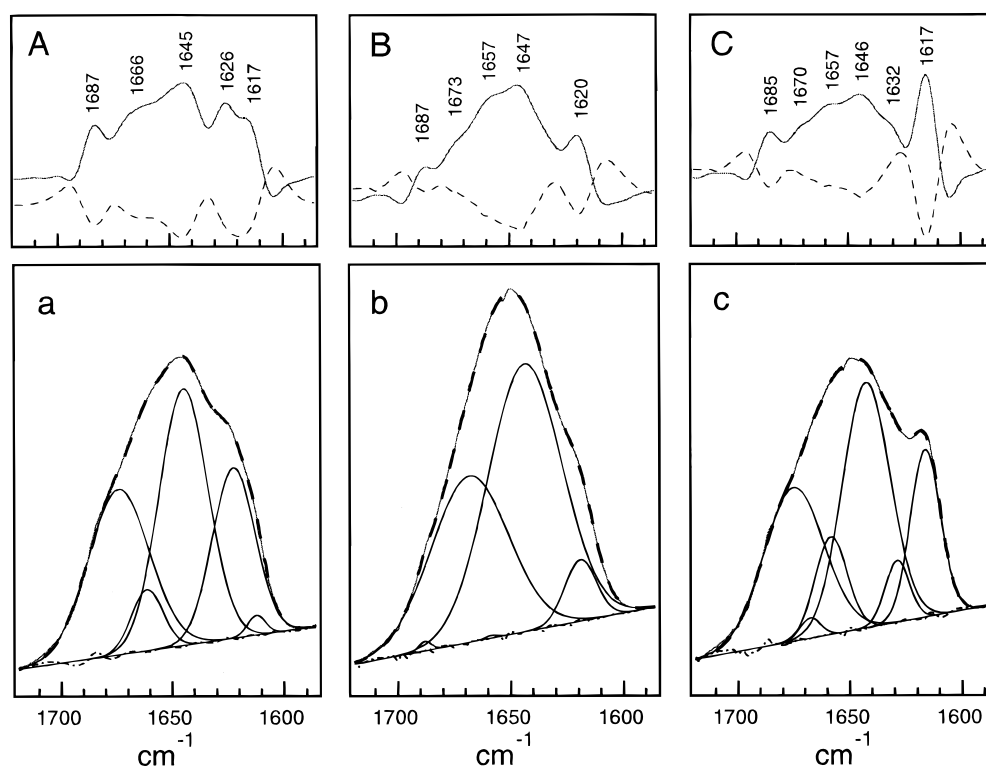


FIGURE 7: Band narrowing and regression analysis of the amide I' line shape of native MSP. Spectra were obtained on the same MSP sample at 20 °C (A and a), after heating to 90 °C (B and b), and after a 1 h additional incubation of the heated sample at 20 °C (C and c). Panels A, B, and C present Fourier deconvolutions (solid line) and second derivatives (dashed line) of the amide I' band. Panels a, b, and c show a comparison of the experimentally determined amide I' line shape (thin solid line) and a reconstruction after regression analysis (thick dashed line). The Gaussian spectral components employed and the residual are also shown.

after cooling that same sample to 20 °C (Figure 7C). In each panel, the Fourier deconvolution of the amide I' band is shown as the solid line; the second derivative of the amide I' band is shown as the dashed line. These methods identify the location of spectral components in the amide I' band as inflection points. In each case, there is good agreement between the results of Fourier deconvolution and second-derivative analysis. We have used these procedures previously in order to identify the number of spectral components and to give initial estimates of their frequencies (35). In Figure 7a–c, we present the results of regression analysis, using the information derived from band narrowing analysis. Bandwidth, frequency, and amplitude of each spectral component were iterated until a minimum in the fit to the experimental data was obtained. The frequencies of the resulting Gaussian spectral components and their amplitudes are given below. The fits are good, as judged by the residuals (Figure 7a–c) and the reduced χ^2 parameters (data not shown).

Correlations have been derived between the frequencies of amide I' spectral components and secondary structural elements in deuterium-exchanged proteins (52–54). Regression analysis of the amide I' line shape of sample 1 is most consistent with one major spectral component at 1653 cm^{-1} (69%). This is a frequency most often assigned to α -helix or to turns/loops. A minor component (4%) at 1642 cm^{-1} is attributable to random structure. Components (12–13%) at 1624 and 1690 cm^{-1} are assignable to β -sheet. A spectral component at 1698 cm^{-1} (2%) was also obtained; the origin of this component is unknown. We conclude that in sample

1, MSP either is primarily α -helical or is organized primarily into loops.

On the other hand, sample 2 shows evidence for a much higher content of random structure (1645 cm^{-1} , 39%), when compared to sample 1. Spectral components at 1612 (1%), 1622 (22%), 1661 (6%), and 1674 (32%) cm^{-1} are also obtained in sample 2. These results are in agreement with our earlier characterizations of native MSP samples (35). As previously described, the variation observed in the line shape of the MSP amide I' band is consistent with considerable variation in secondary structure.

When sample 2 is heated to 90 °C, there is an increase in the amplitude of a spectral component at 1644 cm^{-1} (57%). This result suggests that warming the sample results in an increase (from 39 to 57%) in randomized structure. The amplitude of a spectral feature at 1661–1668 cm^{-1} also increases (6–37%) with increasing temperature. This result suggests an increase in the percentage of turns in native MSP. Spectral components at 1622 (22%) and 1674 (32%) cm^{-1} , assignable to β -sheet and detected at 20 °C, are not detected at 90 °C. At 90 °C, spectral components at 1658 and 1688 cm^{-1} make up less than 1% each of the total area, and a new spectral component at 1619 cm^{-1} (6%) is obtained. Thus, regression analysis suggests that an increase in sample temperature, from 20 to 90 °C, results in conversion of the β -sheet structure to random/turn structural elements. This is evidence for secondary structural changes consistent with thermal denaturation.

On cooling sample 2 from 90 to 20 °C, the amplitudes of spectral features at 1643 and 1668 cm^{-1} , assignable to random structure and turns, decrease to their approximate,

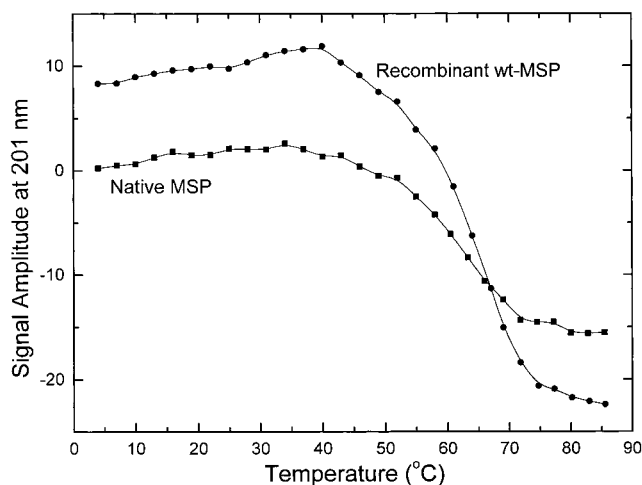


FIGURE 8: Melting curves of native (squares) and recombinant wild-type (circles) MSP. The amplitude of the negative peak at 201 nm, characteristic of the unfolded conformation, was monitored as a function of temperature. Experimental conditions as in Figures 4 and 5 except that the instrument was set to temperature mode.

original values (38% and 1%, respectively). There is a proportionate increase in spectral components assignable to β -sheet (1629 cm^{-1} —5%/ 1675 cm^{-1} —30%) and α -helix/loops (1658 cm^{-1} —10%). An increase in a component at 1616 cm^{-1} (16%) may be due to the formation of intermolecular hydrogen bonds (56), which can be caused by heat-induced aggregation of the sample.

Melting Curves Show That MSP Unfolding by Heat Is Noncooperative. Circular dichroism spectra of MSP unfolded at high temperatures show a minimum at 201 nm (Figures 4 and 5), a feature that is often attributed to random coil (44, 51). Therefore, MSP unfolding was followed as a function of temperature increase by monitoring the signal amplitude at 201 nm (Figure 8). The curves presented in this figure show melting points of 61 and 65 °C for native and recombinant MSP, respectively. The differences in these melting points may reflect secondary structure differences revealed by deconvolutions of the CD spectra of the native and recombinant proteins (Figures 4 and 5, Table 1). The melting curves in Figure 8 also show that neither protein shows extensive cooperativity in its unfolding pattern. Although the melting curves are sigmoidal, the temperature range over which unfolding occurs is very broad ($>30\text{ °C}$) in both cases, which suggests that, in solution, MSP is relatively loosely folded (57).

Near-UV CD Spectroscopy and Size-Exclusion Chromatography Show That MSP Tertiary Structure Is Recovered after Thermal Denaturation. Characterizations of MSP secondary structure by near-UV CD and by FT-IR do not exclude the possibility that heat treatment has permanent effects on tertiary structure. This possibility was examined by near-UV CD spectroscopy and by size-exclusion chromatography. Figure 9 shows the results of the near-UV CD study. Spectra recorded at 25 °C, before and after heating, are nearly identical; the two peaks shown here correspond to tryptophan (294 nm) and tyrosine(s) (285 nm) (51). The CD spectrum recorded at 90 °C did not exhibit these peaks, consistent with thermal denaturation of MSP and the accompanying collapse of its tertiary structure. Similar results were obtained from native MSP samples (not shown). These data indicate that the components of MSP tertiary structure

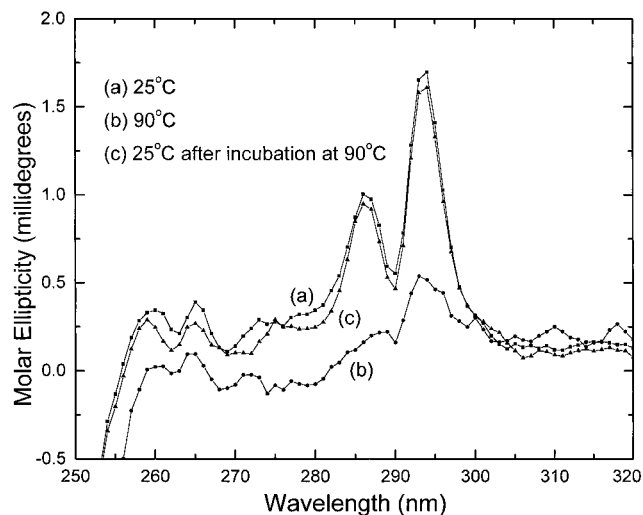


FIGURE 9: Near-UV CD spectra of recombinant MSP recorded at 25 °C (a), 90 °C (b), and 25 °C after 90 °C (c). MSP samples ($25\text{ }\mu\text{M}$ in KH_2PO_4) were thermally equilibrated before scanning. Each spectrum is the average of five scans and was smoothed by a factor of 2. Other experimental conditions: time constant 2 s, bandwidth 1.5 nm, path length 1 cm, scan speed 20 nm/min.

that contribute to the environments of the aromatic amino acids of MSP exhibit reversible behavior. Estimations of the apparent molecular mass of heated samples by gel filtration chromatography verified the results from the near-UV CD study. The apparent molecular mass of all MSP samples was about 41 kDa, regardless of the incubation temperature (data not shown). The high apparent molecular mass of MSP observed here ($\sim 41\text{ kDa}$ instead of the 26.5 kDa predicted from the amino acid sequence) agrees with previous observations (39, 49, 58). These spectroscopic and chromatographic results indicate that the tertiary structure of MSP is not substantially altered by heating and cooling. Taken together with the reconstitution results and far-UV CD and FT-IR results, these data show that MSP's structure and function are not dramatically affected by prolonged incubation of the protein at high temperatures.

DISCUSSION

Although the lack of three-dimensional crystals of MSP has impeded progress toward a full understanding of the relationship between the protein's structure and function, the situation has begun to change as biochemical, biophysical, and molecular biological techniques have been applied to research on MSP [for a recent review, see (7)]. In this paper, we have presented a biochemical and spectroscopic study on the thermostability of native and recombinant spinach MSP. A previous study of MSP, from the thermophilic cyanobacterium *Synechococcus elongatus* (59, see also 33), showed that the cyanobacterial protein's secondary structure was more heat-resistant than that of spinach MSP (59). Effects of heating on the function of spinach MSP were not addressed. Our data (Figure 1) show binding of heat-treated MSP to PSII results in recovery of up to 80% of both O_2 evolution rates (a measure of the efficiency of PSII turnover) and total O_2 yield during prolonged illumination (a measure of the stability of the OEC), relative to an unheated control sample. The ability of MSP to recover its functions on cooling is nearly independent of the time of exposure to high (90 °C) temperature.

Table 2: Properties and Activities of "Natively Unfolded" Proteins

protein	thermostable	% random coil/turns	<i>pI</i>	molecular mass (kDa)		function	reference
				calculated	gel filtration		
MSP	+	4–75 (FT-IR) ^a 45–55 (CD)	5.2	26.5	41	OEC structure/activity	this work
NACP	+	68	6.1	14	58	synapse formation/stabilization	36
Tau	+	>75	10.4	50	600	microtubule binding	65
YP2 β	+	"molten globule"	3–5	11	NA ^b	regulation of RNA translation	50
PKI	+	64	5.3	7.8	22	cAMP-dependent protein kinase inhibitor	61
caldesmon	+	~70	5.7	93	500	Ca ²⁺ -dependent actin–myosin interaction	63, 64
G-substrate	+	N/A	~5.6	23	54	cGMP-dependent kinase substrate	62

^a Reference 35 and this work. ^b Gel filtration data are not available for YP2 β ; SDS–PAGE shows an apparent molecular mass of > 14 kDa.

Figure 1 shows that a modest loss of MSP function occurs rapidly (within 15 min) at the onset of heating, suggesting that MSP must undergo some minor, permanent modifications as soon as it reaches a critical temperature. Protein degradation by heat is not the cause of the small activity loss induced by heating of MSP; Edman analysis of the heated samples resulted in a single N-terminal amino acid sequence (data not shown), identical to that reported for native MSP (42). The C-terminus of MSP is likewise undamaged by heating, because electrophoretic analysis of heated samples gave a single band at the same position as the control sample (data not shown) and gel filtration showed no changes in the apparent molecular mass of heated MSP. If the C-terminus of MSP had been truncated by heating, we would expect it to exhibit a higher mobility on SDS gels and yield a higher molecular mass in gel filtration experiments (49). The most likely cause of the minor loss of MSP function may be irreversible aggregation of the heated protein. Evidence for such aggregation is provided by FT-IR spectroscopy (an increase in intensity in a 1616 cm⁻¹ spectral component of the amide I' band that is observed after heating), although other explanations cannot be ruled out at the present time.

A detailed functional analysis (Figures 2 and 3) indicates that heated native MSP rebinds to PSII and restores activity at stoichiometries similar to those observed with the unheated protein. Figure 3 also shows that after heating, recombinant MSP produces a sigmoidal protein binding curve, and binds adventitiously to PSII as well. As can be seen from the data in this figure, optimal restoration of PSII function is obtained with about 2 mol of heated recombinant MSP/mol of PSII. The observed adventitious binding behavior, therefore, seems to arise from a heat-induced, permanent change in recombinant MSP solution structure that causes it to bind nonspecifically to sites on PSII membranes that are not directly associated with either structure or function of the OEC. The only obvious difference between the native and recombinant proteins arises from the fact that the native MSP has been bound to PSII prior to extraction and purification for use in these experiments. It is not clear why this would cause the differences in PSII binding after heating shown in Figure 3B.

The data in Figures 1–3 demonstrate that MSP from spinach, a mesophile, exhibits a remarkable recovery of native function following heat treatment. Both CD and FT-IR analyses (Table 1 and Figures 6 and 7) show that MSP in solution can adopt a range of predicted secondary structural contents, in agreement with our previous FT-IR

study (35). A comparison of the data in Table 1 and Figures 6 and 7 shows that the predicted secondary structure contents of MSP depend on the method of analysis employed. We are examining the potential causes of these differences, and have addressed some of them in (35). In any case, analyses employing these spectroscopic techniques are consistent in revealing that incubation of MSP at 90 °C results in a loss of secondary structure, consistent with denaturation. Both techniques also confirm that the majority of this structural change is reversible. A more detailed examination of this phenomenon (monitoring ellipticity at 201 nm (Figure 8) shows that heat-induced loss of MSP secondary structure does not occur as a sharp transition, but instead occurs over a broad temperature range (about 35 °C), a result that is taken to indicate that unfolding is not a cooperative process, which would be expected if MSP possessed a compact, highly organized structure (57). Lack of such a compact structure is consistent with the CD (Table 1) and FT-IR (Figures 6 and 7) results indicating that MSP in solution contains ~25% (FT-IR) to as much as 55% (CD) turns and random coil, and with gel permeation data (39, 49) that indicate an anomalously high molecular mass for the protein.

When other properties of the protein are taken into consideration, the unusual heat stability of mesophilic MSP that we document here provides new information on its structure and function. In addition to the high percentage of random coil plus turns in MSP predicted by analysis of CD and FT-IR data, SDS–PAGE and size-exclusion chromatography under nondenaturing conditions show that MSP exhibits a molecular mass much larger than would be expected of a globular protein with a molecular mass of 26.5 kDa (49, 58). A more extensive analysis (60) of the hydrodynamic properties of MSP predicts that the protein possesses an elongated, rather than globular, shape in solution. When combined together with the acidic *pI* of MSP and its thermostability, these other properties form a set of features which have been used to identify and characterize a family of proteins that are described as being "natively unfolded" (36).

Summary information on a selected group of other proteins that belong to the family of "natively unfolded" proteins is shown in Table 2. As can be seen, the functions of these proteins are quite diverse, and include regulation of protein phosphorylation (61, 62), involvement in ribosomal translation (50), synapse formation and stabilization (36), and cytoskeletal function (63–65). Although these are substantially different functions, the proteins in this group share common properties: thermostability, high random coil and

turn content, elongated shapes, and, in most cases, an acidic *pI* (Table 2). In each case, the protein of interest participates in a critically important protein-protein interaction.

"Natively unfolded" solution structures are proposed to provide the conformational flexibility necessary to permit assembly of such proteins into the multisubunit structures of which they are components (36). The observation that MSP is "natively unfolded" conforms to what has been observed about the protein and its interaction with PSII. First, conformational flexibility provides a likely explanation, at least for the present time, for the absence of an MSP crystal structure (57). Second, conformational flexibility in solution may be necessary to expedite functional rebinding of MSP to PSII. We have proposed that MSP assembly into PSII involves a two-step process in which MSP first binds to PSII, after which a reorganization of MSP tertiary structure produces high-affinity binding of the protein (20). If this proposal is correct, then it is likely that the second step requires conformational flexibility for MSP to attain the higher level of secondary structure content detected by isotope editing/FT-IR spectroscopy after the protein has bound to PSII (35). In accord with our proposal for MSP solution structure and assembly into PSII, Enami et al. (66) have recently shown that intramolecular cross-linking of MSP in solution blocks the ability of the protein to reassemble an active OEC; it is possible that cross-linking induces a conformational rigidity to MSP that inhibits the productive binding interactions required for complete restoration of OEC function.

In conclusion, we have provided evidence that MSP exhibits the identifying characteristics of a "natively unfolded" protein. In solution, it appears to be flexible with respect to secondary structure content, as revealed by CD and FT-IR spectroscopy. Like other "natively unfolded" proteins, MSP is resistant to thermal inactivation, and the heat-induced unfolding of MSP is noncooperative. Taken together with evidence that MSP is conformationally flexible in solution, that MSP possesses a significant amount of random structure in solution, and that MSP exhibits anomalous hydrodynamic properties, the demonstration of MSP thermostability leads us to propose that MSP is a new member of the group of "natively unfolded" proteins.

ACKNOWLEDGMENT

We thank Dr. Norma Greenfield for providing the software for CD spectra analysis. R. Hutchison acknowledges support from the Plant Molecular Genetics Institute at the University of Minnesota. Prof. Terry M. Bricker graciously provided preprints of submitted articles. P. A. Brock and R. Boyle are acknowledged for excellent technical assistance.

REFERENCES

1. Debus, R. J. (1992) *Biochim. Biophys. Acta* 1102, 269–352.
2. Bricker, T. M., and Ghanotakis, D. F. (1996) in *Oxygenic Photosynthesis: The Light Reactions* (Ort, D. R., and Yocum, C. F., Eds.) pp 113–136, Kluwer Academic Publishers, Dordrecht, The Netherlands.
3. Nugent, J. H. A. (1996) *Eur. J. Biochem.* 237, 519–531.
4. Kok, B., Forbush, B., and McGloin, M. (1970) *Photochem. Photobiol.* 11, 457–475.
5. Barry, B. A., Boerner, R. J., and dePaula, J. C. (1994) in *The Molecular Biology of the Cyanobacteria* (Bryant, D., Ed.) pp 215–257, Kluwer Academic Publishers, Dordrecht, The Netherlands.
6. Seidler, A. (1996) *Biochim. Biophys. Acta* 1277, 35–60.
7. Bricker, T. M., and Frankel, L. K. (1998) *Photosynth. Res.* 56, 157–173.
8. Britt, R. D. (1996) in *Oxygenic Photosynthesis: The Light Reactions* (Ort, D. R., and Yocum, C. F., Eds.) pp 137–164, Kluwer Academic Publishers, Dordrecht, The Netherlands.
9. Yocum, C. F. (1991) *Biochim. Biophys. Acta* 1059, 1–15.
10. Adelfroth, P., Lindberg, K., and Andreasson, L.-E. (1995) *Biochemistry* 34, 9021–9027.
11. Lindberg, K., and Andreasson, L.-E. (1996) *Biochemistry* 35, 14259–14267.
12. Shen, J.-R., Satoh, K., and Katoh, S. (1987) *Biochim. Biophys. Acta* 933, 358–364.
13. Miyao, M., and Murata, N. (1984) *FEBS Lett.* 170, 350–354.
14. Bricker, T. M. (1992) *Biochemistry* 31, 4623–4628.
15. Miyao, M., Murata, N., Lavorel, J., Maison-Peteri, B., Boussac, A., and Etienne A.-L. (1987) *Biochim. Biophys. Acta* 890, 151–159.
16. Burnap, U. L., Shen, J.-R., Jursinic, P. A., Inoue, Y., and Sherman, L. A. (1992) *Biochemistry* 31, 7404–7410.
17. Razeghifard, M. R., Wydrzynski, T., Pace, R. J., and Burnap, R. L. (1997) *Biochemistry* 36, 14474–14478.
18. Xu, Q., and Bricker, T. M. (1992) *J. Biol. Chem.* 267, 25816–25821.
19. Leuschner, C., and Bricker, T. M. (1996) *Biochemistry* 35, 4551–4557.
20. Betts, S. D., Ross, J. R., Pichersky, E., and Yocum, C. F. (1997) *Biochemistry* 36, 4047–4053.
21. Enami, I., Kaneko, M., Kitamura, N., Koike, H., Sonoike, K., Inoue, Y., and Katoh, S. (1991) *Biochim. Biophys. Acta* 1060, 224–232.
22. Enami, I., Satoh, K., and Katoh, S. (1987) *FEBS Lett.* 226, 161–165.
23. Bricker, T. M., Odom, W. R., and Queirolo, C. B. (1988) *FEBS Lett.* 231, 111–117.
24. Bricker, T. M., and Frankel, L. K. (1987) *Arch. Biochem. Biophys.* 256, 295–301.
25. Frankel, L. K., and Bricker, T. M. (1992) *Biochemistry* 31, 11059–11063.
26. Haag, E., Eaton-Rye, J. J., Renger, G., and Vermaas, W. F. J. (1993) *Biochemistry* 32, 4444–4454.
27. Putnam-Evans, C., Wu, J., Burnap, R. L., Whitmarsh, J., and Bricker, T. M. (1996) *Biochemistry* 35, 4046–4053.
28. Enami, I., Tohri, A., Masaharu, K., Ohta, H., and Shen, J.-R. (1997) *Biochim. Biophys. Acta* 1320, 17–26.
29. Murata, N., Miyao, M., and Kuwabara, T. (1983) in *The Oxygen Evolving System of Photosynthesis* (Inoue, Y., Crofts, A. R., Govindjee, Murata, N., Renger, G., and Satoh, K., Eds.) pp 207–216, Academic Press, Tokyo, Japan.
30. Raval, M. K., Ramaswamy, N. K., and Nair, P. M. (1994) *Plant Sci.* 98, 141–150.
31. Xu, Q., Nelson, J., and Bricker, T. M. (1994) *Biochim. Biophys. Acta* 1188, 427–431.
32. Shutova, T., Irrgang, K.-D., Shubin, V., Klimov, V. V., and Renger, G. (1997) *Biochemistry* 36, 6350–6358.
33. Sonoyama, M., Motoki, A., Okamoto, G., Hirano, M., Ishida, H., and Katoh, S. (1996) *Biochim. Biophys. Acta* 1297, 167–170.
34. Miura, K., Shimazu, T., Motoki, A., Kanai, S., Hirano, M., and Katoh, S. (1993) *Biochim. Biophys. Acta* 1172, 357–360.
35. Hutchison, R. S., Betts, S. D., Yocum, C. F., and Barry, B. A. (1998) *Biochemistry* 37, 5643–5653.
36. Weinreb, P. H., Weiguo, X., Poon, A. W., Conway, K. A., and Lansbury, P. T., Jr. (1996) *Biochemistry* 35, 13709–13715.
37. Berthold, D. A., Babcock, G. T., and Yocum, C. F. (1981) *FEBS Lett.* 134, 231–234.
38. Ghanotakis, D. F., Topper, J., Babcock, G. T., and Yocum, C. F. (1984) *Biochim. Biophys. Acta* 767, 524–531.
39. Betts, S. D., Ross, J. R., Pichersky, E., and Yocum, C. F. (1996) *Biochim. Biophys. Acta* 1274, 135–142.

40. Kuwabara, T., Murata, T., Miyao, M., and Murata, N. (1986) *Biochim. Biophys. Acta* 850, 146–155.
41. Betts, S. D., Hachigian, T. M., Pichersky, E., and Yocum, C. F. (1994) *Plant Mol. Biol.* 26, 117–130.
42. Oh-oka, H., Tanaka, S., Wada, K., Kuwabara, T., and Murata, N. (1986) *FEBS Lett.* 197, 63–66.
43. Betts, S. D., Ross, J. R., Pichersky, E., and Yocum, C. F. (1996) *Biochemistry* 35, 6302–6307.
44. Johnson, W. C., Jr. (1990) *Proteins: Struct., Funct., Genet.* 7, 205–214.
45. Greenfield, N. J. (1996) *Anal. Biochem.* 235, 1–10.
46. Fersht, A. (1977) in *Enzyme Structure and Mechanism*, p 170, W. H. Freeman and Co., New York.
47. Barry, B. A. (1995) *Methods Enzymol.* 258, 303–319.
48. Piccioni, R., Bellemare, G., and Chua, N.-H. (1982) in *Methods in Chloroplast Molecular Biology* (Edelman, M., Hallick, R. B., and Chua, N.-H., Eds.) pp 985–1014, Elsevier, Amsterdam, The Netherlands.
49. Betts, S. D., Lydakis-Simantiris, N., Ross, J., and Yocum, C. F. (1998) *Biochemistry* 37, 14230–14236.
50. Zurdo, J., Sanz, J. M., González, C., Rico, M., and Ballesta, J. P. G. (1997) *Biochemistry* 36, 9625–9635.
51. Kelly, S. M., and Price, N. C. (1997) *Biochim. Biophys. Acta* 1338, 161–185.
52. Susi, H., and Byler, D. M. (1986) *Methods Enzymol.* 130, 290–311.
53. Surewicz, W. F., Mantsch, G. A., and Chapman, D. (1993) *Biochemistry* 32, 389–394.
54. Jackson, M., and Mantsch, H. H. (1995) *Crit. Rev. Biochem. Mol. Biol.* 30, 95–120.
55. Krimm, S., and Bandekar, J. (1986) in *Advances in Protein Chemistry* (Anfinsen, C. B., Edsall, J. T., and Richards, F. M., Eds.) pp 181–364, Academic Press, New York.
56. Clark, A. H., Saunderson, D., and Suggett, A. (1981) *Int. J. Pept. Protein Res.* 17, 353–364.
57. Dobson, C. M. (1992) *Curr. Opin. Struct. Biol.* 2, 6–12.
58. Tanaka, S., and Wada, L. (1988) *Photosynth. Res.* 17, 255–266.
59. Motoki, A., Miura, K., Shimazu, T., Kanai, S., Hirano, M., and Katoh, S. (1992) in *Research in Photosynthesis* (Murata, N., Ed.) Vol. II, pp 413–416, Kluwer Academic Publishers, Dordrecht, The Netherlands.
60. Zubrzycki, I. Z., Frankel L. K., Russo, P. S., and Bricker, T. M. (1998) *Biochemistry* 37, 13553–13558.
61. Thomas, J., van Patten, S. M., Howard, P., Day, K. H., Mitchell, R. D., Sosnick, T., Trewhella, J., Walsh, D. A., and Maurer, R. A. (1991) *J. Biol. Chem.* 266, 10906–10911.
62. Aswad, D. W., and Greengard, P. (1981) *J. Biol. Chem.* 256, 3487–3493.
63. Lynch, W. P., Riseman, V., and Bretscher, A. (1987) *J. Biol. Chem.* 262, 7429–7437.
64. Bretscher, A. (1984) *J. Biol. Chem.* 259, 12873–12880.
65. Schweers, O., Schönbrunn-Hanebeck, E., Marx, A., and Mandelkow, E. (1994) *J. Biol. Chem.* 269, 24290–24297.
66. Enami, I., Kamo, M., Ohta, H., Takahashi, S., Miura, T., Kusayanagi, M., Tanabe, S., Kamei, A., Motoki, A., Hirano, M., Tomo, T., and Satoh, K. (1998) *J. Biol. Chem.* 273, 4629–4634.

BI981847Z